CS754 PROJECT REPORT

Saumya Goyal, Parth Laturia

21 June 2020

1 Problem Statement

Computed Tomography for medical procedures involves the risk of exposing the person to a high amount of radiation which is not recommended. A common solution to the problem is to consider radon projections on fewer angles. We implement the paper titled "Low radiation tomographic reconstruction with and without template information" which proposes a solution with reduced intensity of X-rays as compared to reduced number of angles. In the case discussed in the paper, the measurement is denoted by the equation

$$\mathbf{y} \sim Poisson(I_0 e^{-\Phi\Psi x}) + \eta \tag{1}$$

Here, I_0 can be a matrix if intensity is different for different bins. η represents Gaussian noise with standard deviation σ.

We specifically focus on prior based reconstruction in our project which considers previously obtained high dose measurements as templates for reconstruction.

2 Algorithms Implemented

Template based reconstruction involves several steps which we outline here below

2.1 Computation of Weights Map

Weights map forms the main component of the optimisation procedure implemented in the paper. It is a matrix which helps us in determining locations in the sample which may be different from templates. Algorithm followed for computation of the weights map, given the radon projections of templates and the low-dose projection of test sample is:

1. **Projecting the test measurements onto the template eigenspace**: We create a vector space from eigenvectors of projections of templates for each projection angle. We only select the eigenvectors corresponding to

the top eigenvalues here. Eigenvectors with eigenvalues lesser than 10^{-18} were usually ignored. The projections of the test sample ($\boldsymbol{y}$) are projected onto this eigenspace for each angle to form the projection $\boldsymbol{y_p}$

2. **Probability of change in each bin**: The values $\boldsymbol{h} = \sqrt{\boldsymbol{y} + (3/8) + \sigma^2} - \sqrt{\boldsymbol{y_p} + (3/8) + \sigma^2}$ should be samples from $\mathcal{N}(0, 1/4)$ if the test sample does not differ from the templates in corresponding bins. This result comes from the *General Anscombe Transform*. We use z-test on $\boldsymbol{h}$ to determine probability of no change in each bin. This forms the matrix p.

3. **Deriving the weights map from probability matrix**: We implemented the approach discussed in the paper for computation of weights map. The approach, as well as our modification to the approach are discussed below.

2.1.1 Inverse projection of probability matrix

The approach discussed in the paper involves inverse radon projection of the p-values matrix followed by inversion and linear stretching to obtain the weights map. We are happy to to comment here, that we were able to point out a misprint to the authors regarding this. The inverse projection step described above was to be done on the $(1 - \boldsymbol{p})$ matrix rather than $\boldsymbol{p}$.

2.1.2 Validity of inverse projection and our suggestion

Summation of values along a particular line form the value of the kth bin in a radon projection for the jth angle. Let the indices of the pixels present in the "line" corresponding to the kth bin in the jth angle be present in a vector $\boldsymbol{R_{jk}}$. Now the p-values matrix contains probability of no change in each bin. This should equal to product of probability of no change in each pixel($\boldsymbol{r}$) if we assume that probability of change in a pixel is independant of it's neighbours:

$$p_{jk} = \prod_{i \in R_{jk}} r_i \tag{2}$$

Now the $(1 - \boldsymbol{p})$ matrix does not have a good representation as sum of probabilites by the inclusion-exclusion principle. Inverse projection of the matrix might only approximately highlight areas of change.
Instead of this, we propose doing inverse projection on the element wise logarithm of the p-values matrix. By the above equation, element wise exponentiation of the obtained matrix will result in a matrix containing probabilities of no change in each pixel. We believe this matrix might be a better representation of a weights map.
We were unable to develop methods to produce better contrast between regions of high and low probability because of limitations in time and our experience in the field.

2.2 Re-irradiation

This step involves applying high dose X-rays onto the bins corresponding to more changes in the projection space. We separate the bins corresponding to probabilities of no change lesser than a particular limit. This limit was decided differently for different datasets depending on the ratio given in the paper. Higher intensity projection was simulated for these separated bins. Intensity values now form a matrix denoting different intensities for different bins as described below equation (1).

2.3 Minimisation

We perform optimisation using the cost function:

$$\boldsymbol{J(\theta, \alpha)} = \sum \frac{(\boldsymbol{y} - \boldsymbol{I}e^{-\Phi\Psi\theta})^2}{(\boldsymbol{I}e^{-\Phi\Psi\theta} + \sigma^2)} + \lambda_1||\boldsymbol{\theta}||_1 + \lambda_2||\boldsymbol{W}(\Psi\theta - (\mu + V\boldsymbol{\alpha}))||_2^2 \quad (3)$$

Note that we use a bold I here to denote intensity as a matrix which may be uniform or non-uniform depending on whether the optimisation is being done with or without re-irradiation. V is the matrix of eigenvectors corresponding to significant eigenvalues of the template data in the *image* space. Similarly, μ is the mean of the templates in the image space.

The parameters λ_1 and λ_2 were chosen omnisciently by the process described in the next section.

The cost function is minimised using alternate minimisation on $\boldsymbol{\theta}$ and $\boldsymbol{\alpha}$ until convergence is reached. We use a slightly modified version of Fast Iterative Shrinkage Thresholding Algorithm present at https://github.com/tiepvupsu/FISTA with the condition of non-negativity of $\Psi\theta$ imposed. This condition is necessary to ensure the sanity of the reconstructed image which can not have negative values at any pixel.

2.4 Parameter Tuning

First, we do a kind of binary search approach to find a broad range (of width around 1-2) that will contain the optimal value of λ_1. Then, to fine tune the parameter λ_1 and find the optimal value of λ_1 more accurately and precisely, we involve 2 equations mentioned below:

$$\boldsymbol{J(\theta, \alpha)} = \sum \frac{(\boldsymbol{y} - \boldsymbol{I}e^{-\Phi\Psi\theta})^2}{(\boldsymbol{I}e^{-\Phi\Psi\theta} + \sigma^2)} + \lambda_1||\boldsymbol{\theta}||_1 \quad (4)$$

$$D = abs(||\frac{(\boldsymbol{y} - \boldsymbol{I}e^{-\Phi\Psi}\theta)}{\sqrt{(\boldsymbol{I}e^{-\Phi\Psi\theta} + \sigma^2)}}||_2 - \sqrt{m}) \quad (5)$$

Over the broad range obtained, we iterate over different values of λ_1 spaced uniformly. For each value, we compute the optimal θ that minimises the cost function in Equation 4, evaluate D on corresponding to this θ. Using this

technique, we find the λ_1 whose θ resulted in the smallest value of D. This λ_1 obtained is our optimal λ_1. This method involves working over statistical principles pertaining to the Poisson or the Poisson-Gaussian noise model.

3 Datasets Used

We tested our implementation using the Okra, Potato and Sprouts dataset used in the paper. We performed reconstruction on 2D slices which best highlighted the difference in the samples by visual inspection. Due to memory limitations we picked patches of sizes upto 140×140 from the chosen slices of all the templates focusing on the regions showing the change significantly.

4 Results

We present the images of the reconstructed slices along with their RMSE values with respect to the corresponding slices:

4.1 Okra

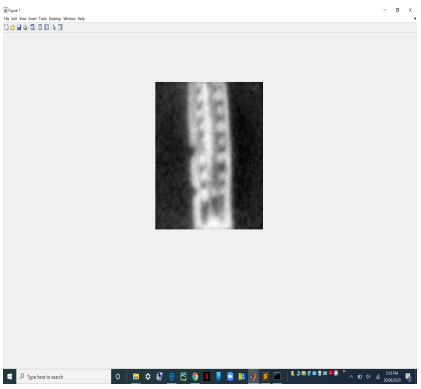

(a) Without Irradiation

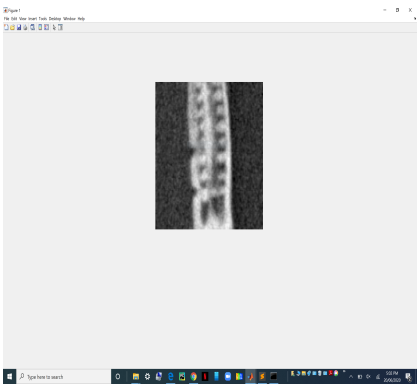

(b) With Irradiation

4.1.1 Without Re-irradiation

RMSE = 0.2404, Optimal $\lambda_1 = 6.2$, Optimal $\lambda_2 = 700$

4.1.2 With Re-irradiation

RMSE = 0.1837, Optimal $\lambda_1 = 6.9$, Optimal $\lambda_2 = 700$

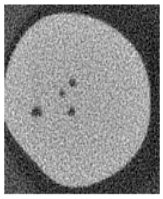

(a) Without Irradiation

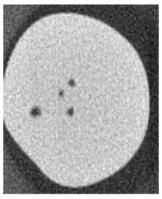

(b) With Irradiation

4.2 Potato

4.2.1 Without Re-irradiation

RMSE = 0.2404, Optimal λ_1 = —, Optimal λ_2 = 700

4.2.2 With Re-irradiation

RMSE = 0.1837, Optimal λ_1 = —, Optimal λ_2 = 700

4.3 Sprouts

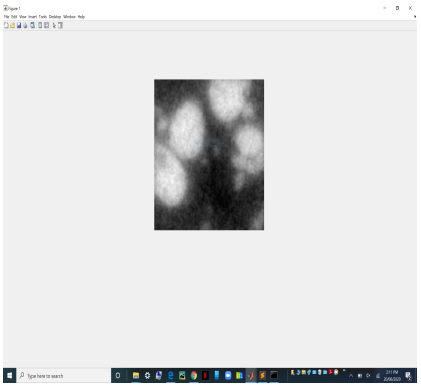

(a) Without Irradiation

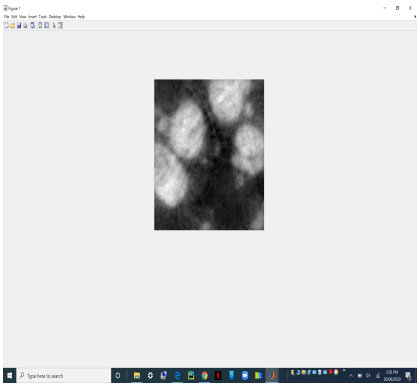

(b) With Irradiation

4.3.1 Without Re-irradiation

RMSE = 0.2404, Optimal λ_1 = 3.5, Optimal λ_2 = 700

4.3.2 With Re-irradiation

RMSE = 0.1837, Optimal $\lambda_1 = 4.0$ Optimal $\lambda_2 = 700$

5 Conclusion and Future Possibilities

As observed from the reconstructed data, we are able to achieve low RMSE values while reconstructing even with low intensity data. These are promising results for medical imaging. With high intensity radiation on only small regions of change we are able to achieve even lesser RMSE values.
Our implementation involves a considerably large number of parameters *vis-a-vis* patch size for z-test, high and low values of intensity chosen for the dataset, λ_1, λ_2, normalisation of input data, number of eigen vectors chosen, etc. These highly affect the quality and accuracy of reconstruction. We have the possibility of manually tuning these parameters to obtain 'good' reconstruction results. In a practical scenario we might not have the changing parameters like intensity values after reconstruction to obtain optimal results. Though we do not have techniques to determine values of such parameters prior reconstruction, development on this front can help greatly for medical applications as well as for providing good theoretical bounds on the accuracy of the reconstruction.
An important shortcoming of the approach employed in the project could be poor reconstruction of slices very different from templates. A low-valued weights map might remove our ability to extract much from One additional shortcoming of our implementation of the project was that we were unable to perform reconstruction on entire slices due to memory limitations.

5.1 Merits of the Project

- Our implementation has considerably large number of parameters that determine the quality and accuracy of the reconstruction, *vis-a-vis* patch size, I_{low}, I_{high}, λ_1, λ_2, normalized sum, number of eigen vectors considered for reconstruction. Hence, our model is flexible and adaptive to changes and not rigid. So there is a great scope of modifying them such that our algorithm gets adjusted to produce accurate reconstruction for any general data-set easily. Hence, we were able to change these parameters flexibly so that we get the best possible reconstruction.

5.2 Shortcomings of the Project

- Due to memory issues, our implementation is not able to return the reconstructed image of the whole slice.
- The values of the parameters considerably varies over the data-set.